



HAL
open science

A ZeroPower DC voltage-to-RF impedance converter enabling sustainable & frugal wireless sensor networks

Raphael Dauny, Simon Hemour, Corinne Dejous, Xiaoqiang Gu

► To cite this version:

Raphael Dauny, Simon Hemour, Corinne Dejous, Xiaoqiang Gu. A ZeroPower DC voltage-to-RF impedance converter enabling sustainable & frugal wireless sensor networks. 2024 European Microwave Conference, Sep 2024, Paris, France. hal-04559996

HAL Id: hal-04559996

<https://hal.science/hal-04559996>

Submitted on 26 Apr 2024

HAL is a multi-disciplinary open access archive for the deposit and dissemination of scientific research documents, whether they are published or not. The documents may come from teaching and research institutions in France or abroad, or from public or private research centers.

L'archive ouverte pluridisciplinaire **HAL**, est destinée au dépôt et à la diffusion de documents scientifiques de niveau recherche, publiés ou non, émanant des établissements d'enseignement et de recherche français ou étrangers, des laboratoires publics ou privés.

A ZeroPower DC voltage-to-RF impedance converter enabling sustainable & frugal wireless sensor networks

Raphaël Dauny^{#1}, Xiaoqiang Gu^{*2}, Corinne Dejous^{#3}, Simon Hemour^{#4}

[#]IMS Laboratory, CNRS UMR 5218, Bordeaux INP, University of Bordeaux, France

^{*}EEME School, University of Bristol, Bristol, UK

{¹raphael.dauny, ³corinne.dejous, ⁴simon.hemour}@u-bordeaux.fr ; {²sean.gu}@bristol.ac.uk

Abstract — Amidst climate change and raw material shortages that begin to impact our society, the crucial role of engineers is to invent tools that enable citizens to regulate their footprint. Field sensors associated with control engineering have proven so far to be a very effective way to save energy. Unfortunately, many "smart sensors" are deployed today at a huge footprint cost (the global impact of carbon footprint in the electronics industry is currently larger than the traditional car and truck industry and is still rising). This paper introduces a way to turn any DC voltage sensors -- with a special emphasis on frugal sensors -- into wireless systems towards the dawn of sustainable wireless sensor networks.

A proof of principle is reported with a theoretical backscattering operation distance of 20 m (at -15 -dBm input), and with input sensor voltage down to 300 mV, yielding 19% modulation depth for backscattering.

Keywords — backscattering, rectifier, Schottky diodes, wireless sensing, zero-power

I. INTRODUCTION

In today's era of profound global transformation, marked by the urgent imperative to mitigate energy consumption and reduce carbon footprints, sensors emerge as indispensable instruments for our society's sustainable evolution. Wireless operation offers sensors enhanced flexibility, scalability, and deployment ease, embodying the ethos of sustainability by minimizing physical infrastructure and resource consumption. However, achieving truly wireless functionality remains a challenge, primarily due to energy dependency, which, in today's wireless sensor network, often necessitates a wired power connection or regular battery replacement. To address this challenge, we must pursue two complementary paths:

The first avenue entails the ongoing development of micro-energy generators (more commonly called Energy Harvesters), a field that has seen extensive research spanning several decades [1-2]. These generators hold the promise of harnessing ambient energy sources to power net-zero-power sensors microsystems, reducing reliance on traditional power sources and minimizing environmental impact.

Simultaneously, the exploration of zero-power communication using backscattering technology presents an underutilized solution with far-reaching sustainability implications. Originally employed for covert surveillance purposes [3], backscattering technology enables devices to communicate by modulating the reflection of an incident radiofrequency (RF) signal back to the transmitter. By eliminating the need for active power sources during

communication, backscattering minimizes energy consumption and environmental footprint.

Numerous backscattering strategies have been proposed [4-6], each offering unique advantages in terms of power efficiency and environmental impact. Passive RF transduction sensors, commonly referred to as LC resonators, have emerged as a particularly promising avenue [7], [8]. These sensors leverage the temporal change in inductance or capacitance to modulate the reflection coefficient of the resonator, generating a backscattered signal without the need for active power sources. However, the custom fabrication of resonators with high-quality factors presents challenges, which may sometimes translate into high carbon footprint fabrication.

On the contrary, frugal sensors are cost-effective, simple, and resource-efficient. This class of sensors was developed to meet the needs of resource-constrained environments and have intrinsically a low carbon footprint. However, because low-cost materials are used, frugal sensors are usually lossy and inappropriate for RF use.

Furthermore, many passive sensors operate at very low frequencies, utilizing resistance variation due to time-varying physical phenomena such as force, strain, or light. Despite their rare counter-example [9], these sensors lack the capability to low RF current flow due to their sizeable footprint and lengthy connection cables.

In this context, our paper introduces a net-zero power circuit based on the trans-frequency impedance converter, capable of converting ultra-low DC voltage variations into RF impedance changes without any power supply voltage (Vdd). It can be used to transform any passive wired sensor (photodiode, piezoelectric, induction sensors, dynamo-like sensors, solar cell...) or any device and circuit that would provide low-frequency ultra-low voltage signal into wireless backscattering sensors.

II. DC VOLTAGE TO IMPEDANCE CONVERTER

The voltage-to-impedance converter generic schematic and its operation are depicted in Figs. 1(a) and 1(b), respectively. It involves a diode to rectify the illumination power remotely transmitted to activate the sensor. (RF-to-DC power conversion). The resulting DC voltage is used to bias a transistor utilized as a voltage-controlled resistor (VCR). Note that the diode acts as a DC current generator, effectively self-biased by its current. Upon applying a control voltage (coming from a sensor) to the gate of the transistor, the overall resistance

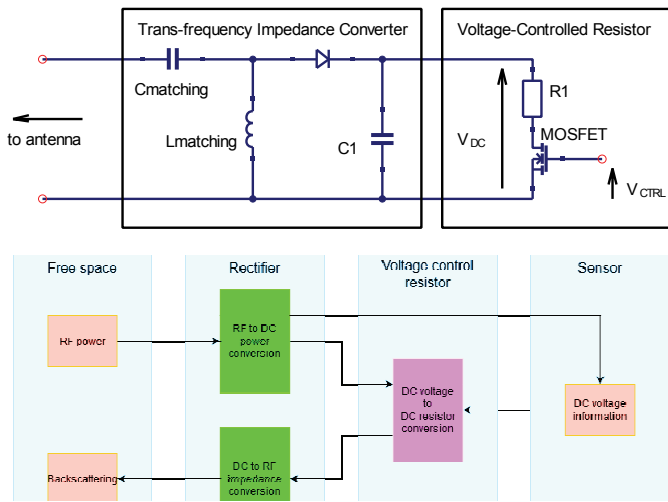


Fig. 1. (a) Simplified schematic of the proposed circuit, composed of a trans-frequency impedance converter and a voltage controlled resistor. (b) Typical operation: The remote illumination RF power is rectified by the diode, which generates a local DC voltage. This DC voltage is used to bias a voltage-controlled resistor (and could eventually bias a sensor), that perform load modulation based on V_{CTRL} .

loading the DC current generator is changing, thus shifting the DC self-bias point of the diode (see Fig. 2). Since the RF impedance seen from the antenna is in part set by the first derivation of the diode $I(V)$ exponential curve at the operating point as shown in Fig.2, a change of self-bias condition will impact the RF impedance (DC-to-RF impedance conversion), which is why rectifier circuit can be seen as trans-frequency impedance converters. The overall operation of the circuit will now be reported stage by stage.

A. Rectifier circuit

As shown in the first block of Fig. 1(a), the rectifier circuit is based on an SMS7630 Schottky diode, well known for its nonlinear performances at low input power [10-13]. It is matched by two components, $C_{matching}$ and $L_{matching}$, which also act as a bias tee for the self-biasing operation of the circuit. The capacitor $C1$ is placed after the diode and acts both as low-pass filter for the rectified voltage, and to ground the diode at RF frequencies.

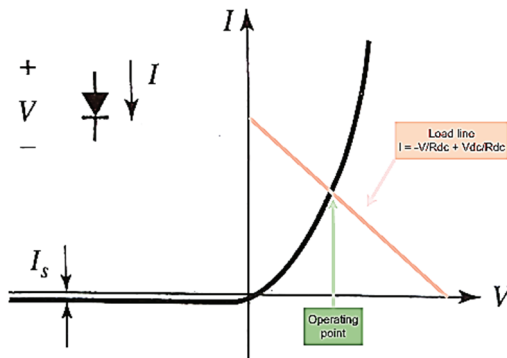


Fig. 2. Typical diode current-voltage dependency. Since the RF impedance is set by the derivative of the curve at the operating point, a change in DC self-bias condition will yield a change in its RF impedance.

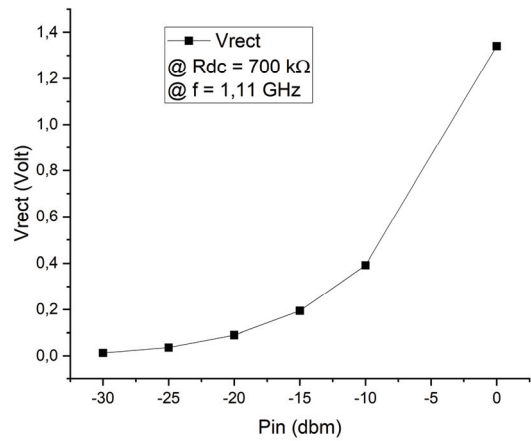


Fig. 3. DC voltage generated by the rectifier diode upon the application of a continuous was RF power. An unrealistic measurement at -5dBm has been removed. The measurement is done at 1.11GHz for a DC load resistance close to open circuit conditions ($R_{DC}=700\text{k}\Omega$)

As shown in Fig. 3, the open-circuit voltage varies quasi-quadratically with the input power, which corresponds to the regular behaviour of a diode-based power detector.

B. DC voltage control to DC resistor conversion

The key feature of this proposed design is the low-voltage operation, i.e. no more than hundreds of millivolts. For this reason, N-Channel 0.2V threshold EPAD ALD110800 MOSFET from *Advanced Linear Devices* is chosen. The circuit is shown in the second block of Fig. 1(a). The transistor regulates the flow of electrons in its channel through the potential difference between its source and gate pins, controlled by the voltage V_{CTRL} (Fig. 4). Ohm's law symbolises the coefficient linking current to voltage as the resistance. Nonetheless, the change in gate voltage modifies the amount of current flowing through the device. Maintaining a constant voltage V_{DC} is equivalent to adjusting the coefficient linking voltage and current, which leads to a variation in the transistor's equivalent resistance. Fig. 5 shows the influence of the control voltage V_{CTRL} on the equivalent resistance of the VCR circuit, R_{dc} . The measurements are carried out with the VCR connected to the rectifier (Fig. 1(a)) and show a variation of the synthesized resistance for different values of RF input power.

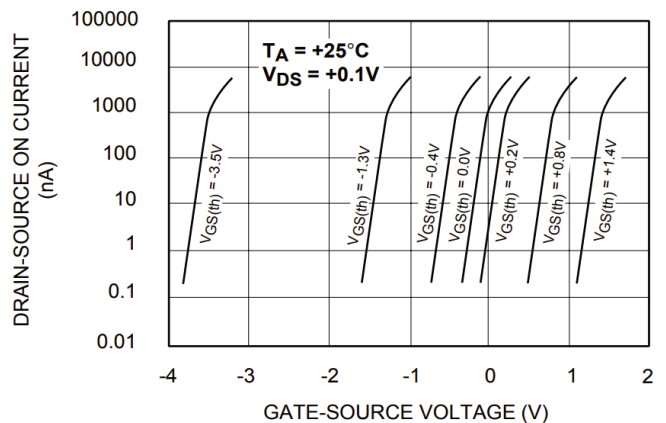


Fig. 4. Subthreshold forward transfer characteristics of the ALD110800 MOSFET from *Advanced Linear Devices* [14].

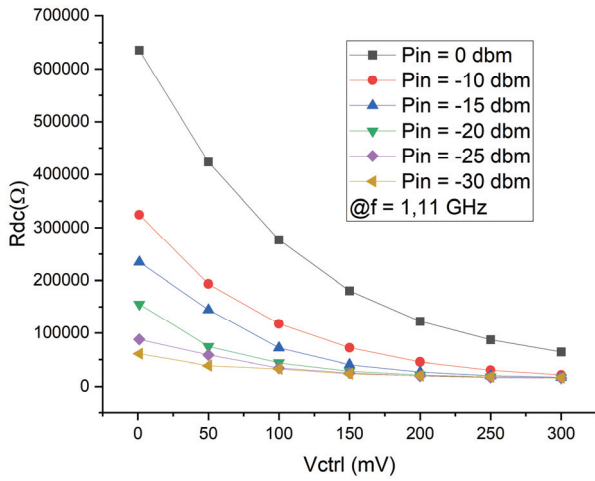


Fig. 5. Equivalent DC resistor as function of voltage control to input power rectifier from -30 dBm to 0 dBm and an input frequency of 1.11 GHz.

The variation in equivalent resistance depends on the input power, as it is directly linked to the voltage V_{dc} supplied by the rectifier. It is also noted that the energy supplied by the rectifier is directly linked to the diode bias point, which depends on the load associated with the rectifier.

The measurements in Fig. 5 show that the DC resistor varies inversely with the control voltage and has a range of variation increasing with the input RF power. In the prototype, the resistor R_1 (10 k Ω) is included as a pull resistor to observe the current flowing through the circuit and deduce its equivalent resistance. Unfortunately, it has been understood after the measurements campaign that this resistor is setting the floor limit of the VCR, and should be removed for optimum operation.

C. DC resistor to RF impedance conversion

To yield a large backscattering modulation power, the converter needs to exhibit large “transformation sensitivity” – which is defined as the ratio between RF impedance variation over DC resistance variation. It is shown in Fig. 6, that diode junction resistor R_j can be seen as the link between the DC and RF domains for the diode. The DC equivalent circuit provides the load line, clearly visible in a solid red line in Fig. 2, which determines the operating point of the diode, represented by the intersection of the two curves.

The DC conductance of the diode G_j (which is the inverse of the resistance R_j in the circuit shown in Fig. 5) is calculated by taking the derivative of the characteristic curve $I(V)$ of the diode, evaluated at its operating point.

$$\frac{dI}{dV} = G_j = \frac{1}{R_j} \quad (1)$$

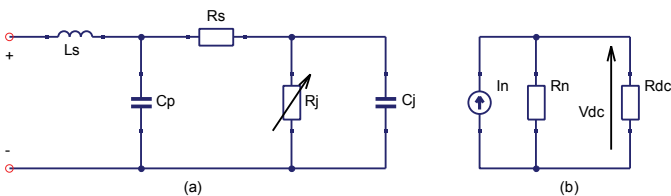


Fig. 6. Equivalent circuit of the Schottky diode in (a) AC domain (b) DC domain by Norton model. The diode is loaded in DC with R_{dc} resistor.

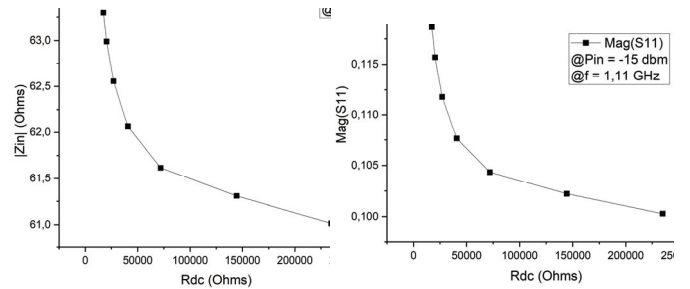


Fig. 7. (a) Reflection coefficient at the input port of the circuit, corresponding to ratio of power being reflected back to the antenna, as a function of DC load resistance variation. (b) Magnitude of the input impedance of the circuit as a function to DC load resistance variation. Both measurements are done with an input signal of 1.11 GHz, with a power of -15 dBm.

This operating point dependent on the load resistance R_{dc} highlights a link between the impedance seen at the input of the RF system and the DC resistance that makes it up. By adjusting the value of R_{DC} , The RF impedance of the system can be directly changed. The measurement shown in Fig. 7(a) highlights the relationship between the load resistance and the RF impedance created by the rectifier. An exponential behaviour is observed between the load resistance and the RF impedance. This result is consistent with the theoretical study, since the resistance R_j is related to the inverse of the derivative of the diode’s $I(V)$ curve, representing an exponential function.

Fig. 7(b) shows that the variation of the load resistance impacts the amount of energy reflected by the system. Therefore, it is possible to deduce the variation in DC loads by observing the variation in RF energy reflected from the system. This link between load variation and reflected RF energy provides an ideal metric for evaluating and adjusting system parameters.

While the practical parameter defining the amount of backscatter power is the Reflection coefficient, it might not be the most useful parameter to analyze. In fact, the reflection coefficient is very much dependent on the matching circuit. It

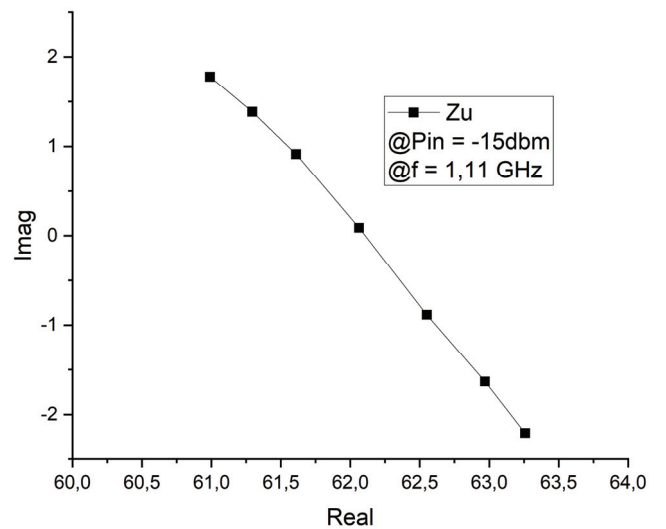


Fig. 8. Input impedance distribution to a voltage control changes from 1 mV to 300 mV (the point corresponding to 1 mV is furthest to the left, while the data corresponding to 300 mV is furthest right). Measurements are done with an input RF power of -15 dBm, for a continuous wave of 1.1 GHz.

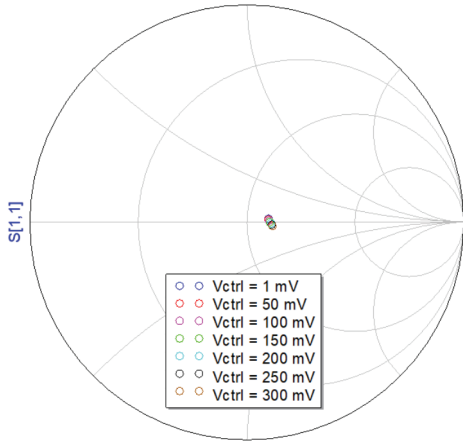


Fig. 9. Reflection coefficient distribution (measurement) when a voltage control changes from 1 mV to 300 mV to an input power of -15 dBm and frequency of 1.11 GHz.

is, therefore, instructive to look at the raw RF impedance seen from the antenna (Fig. 8).

Therefore, rather than looking at the maximum reflexion coefficient variation [15-16], it is useful to optimize first the system for maximum RF complex impedance variation before working on the matching circuit.

III. CONCLUSION

Figure 9 shows the RF input impedance system variation on the Smith chart for different DC control voltage V_{CTRL} , while the system is illuminated at 1.11 GHz, and the received power is -15 dBm. The maximum reflection coefficient variation is $\Delta\Gamma = 3.5\%$, while the mean S_{11} is $\langle \Gamma \rangle = 10.7\%$, which yields a reflected signal in AM modulation with $\Delta\Gamma / (2 \cdot \langle \Gamma \rangle) = 19\%$ modulation depth.

To evaluate this work and enable comparison for future work, we suggest computing the ratio of $\Delta\Gamma$ as a function of control voltage. To this end, Fig. 10 links the variation of V_{CTRL} and that of Gamma. Our results show that an almost linear relationship is obtained between these two values (the former two exponential behaviour compensating each other). The sensitivity of this demonstrator is small (0.14 V^{-1}), but demonstrates the feasibility of the concept. It can be enhanced

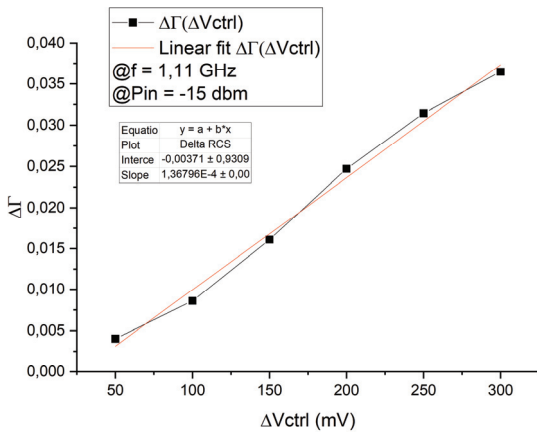


Fig. 10. Reflection coefficient variation as function a voltage control variation starting from 1 mV to an input power of -15 dbm and frequency of 1.11 GHz.

by optimizing the diode circuit and the VCR to reach lower resistance values. A pre-amplification of V_{CTRL} could also enhance the sensitivity. Note that the low power operations limits we assigned to this work (low V_{CTRL} and low input power) can be exceeded, yielding far better performances. However, this work aimed at demonstrating the feasibility of considering long-distance RF illumination (-15 -dBm input power corresponds to 31 mW and about 20 m of theoretical free space operational distance according to Friis equation with a 36-dBm EIRP source at 956 MHz, a transmitter antenna gain of 5 dB and a receiver antenna gain of 2 dB).

IV. ACKNOWLEDGEMENT

The author would like to thank JL Lachaud for fruitful discussion and acknowledge the funding of R.D. from the grants ANR-21-CE19-0015-01, and UB RRI BEST.

REFERENCE

- [1] K. Niotaki *et al.*, "RF Energy Harvesting and Wireless Power Transfer for Energy Autonomous Wireless Devices and RFIDs," *IEEE J. Microw.*, vol. 3, no. 2, pp. 763-782, Apr. 2023.
- [2] FK. Shaikh, and S. Zeadally, "Energy harvesting in wireless sensor networks: A comprehensive review," *Renew. Sustain. Energy Rev.*, vol. 55, pp. 1041-1054, Mar. 2016.
- [3] P. Nikitin, "Leon Theremin (Lev Termen)," *IEEE Antennas Propag. Mag.*, vol. 54, no. 5, pp. 252-257, Oct. 2012.
- [4] B. Kellogg, A. Parks, S. Gollakota, J. R. Smith, and D. Wetherall, "Wi-Fi backscatter: Internet connectivity for RF-powered devices," in *Proc. ACM SIGCOMM*, Chicago, IL, USA, Jun. 2014, pp. 607-618.
- [5] R. Correia, N. B. Carvalho, and S. Kawasaki, "Continuously Power Delivering for Passive Backscatter Wireless Sensor Networks," *IEEE Trans. Microw. Theory Tech.*, vol. 64, no. 11, pp. 3723-3731, Nov. 2016.
- [6] X. Tang, G. Xie, and Y. Cui, "Self-Sustainable Long-Range Backscattering Communication Using RF Energy Harvesting," *IEEE Internet Things J.*, vol. 8, no. 17, pp. 13737-13749, Sept. 2021.
- [7] Q. A. Huang, L. Dong, and L. F. Wang, "LC Passive Wireless Sensors Toward a Wireless Sensing Platform: Status, Prospects, and Challenges," *J. Microelectromechanical Syst.*, vol. 25, no. 5, pp. 822-841, Oct. 2016.
- [8] K. S. V. Idhiam, P. D. Pozo, K. Sabolsky, E. M. Sabolsky, K. A. Sierros, and D. S. Reynolds, "All-Ceramic LC Resonator for Chipless Temperature Sensing Within High Temperature Systems," *IEEE Sens. J.*, vol. 21, no. 18, pp. 19771-19779, Sept. 2021.
- [9] H. Ribeiro, S. Hemour, and N. B. Carvalho, "Fully Passive Modulation Technique for SWIPT Scenarios," in *Proc. IEEE MTT-S Int. Microw. Symp.*, San Diego, CA, USA, Jun. 2023, pp. 999-1002.
- [10] S. Hemour *et al.*, "Beyond Rectification: Passive Backscattering Modulation," in *Proc. Wireless Power Transfer Conference and Expo*, Kyoto, Japan, pp. 1-4, May 2024.
- [11] X. Gu, S. Hemour, and K. Wu, "Far-Field Wireless Power Harvesting: Nonlinear Modeling, Rectenna Design, and Emerging Applications," *Proc. IEEE*, vol. 110, no. 1, pp. 56-73, Jan. 2022.
- [12] X. Gu, S. Hemour, L. Guo, and K. Wu, "Integrated Cooperative Ambient Power Harvester Collecting Ubiquitous Radio Frequency and Kinetic Energy," *IEEE Trans. Microw. Theory Tech.*, vol. 66, no. 9, pp. 4178-4190, Sept. 2018.
- [13] X. Gu, L. Guo, S. Hemour, and K. Wu, "Optimum Temperatures for Enhanced Power Conversion Efficiency (PCE) of Zero-Bias Diode-Based Rectifiers," *IEEE Trans. Microw. Theory Tech.*, vol. 68, no. 9, pp. 4040-4053, Sept. 2020.
- [14] Advanced Linear Devices, "ALD110800APCL- MOSFET", [online], <https://www.aldinc.com/pdf/ALD110800.pdf>.
- [15] A. Voisin, A. Dumas, N. Barbot, and S. Tedjini, "Differential RCS of Multi-State Transponder," in *Proc. Wirel. Power Week*, Bordeaux, France, Jul. 2022, pp. 195-198.
- [16] N. Barbot, O. Rance, and E. Perret, "Classical RFID Versus Chipless RFID Read Range: Is Linearity a Friend or a Foe?," *IEEE Trans. Microw. Theory Tech.*, vol. 69, no. 9, pp. 4199-4208, Sept. 2021.